

The Potential of a Spaceborne Cloud Radar for the Detection of Stratocumulus Clouds

NEIL I. FOX AND ANTHONY J. ILLINGWORTH

JCMM, Department of Meteorology, University of Reading, Reading, United Kingdom

(Manuscript received 4 January 1996, in final form 22 July 1996)

ABSTRACT

The radar reflectivity and liquid water content of stratocumulus clouds have been computed from cloud droplet spectra recorded during more than 4000 km of cloud penetrations by an aircraft, and the probability of detecting various values of liquid water content as a function of the radar sensitivity threshold has been derived. The goal of the study is to specify the sensitivity required for any future spaceborne cloud radar. In extensive marine stratocumulus deeper than about 200 m, occasional but ubiquitous drizzle-sized droplets of up to 200 μm dominate the radar return and increase it by between 10 and 20 dB above the cloud droplet contribution to the return, making radar detection easier, although the concentration of the drizzle drops is so low that they have no effect on the liquid water content or effective radius. These occasional drizzle-sized droplets are present throughout the vertical and horizontal extent of such clouds but should evaporate within 200 m of cloud base. On occasion, the drizzle can fall farther and may yield a false measurement of cloud-base altitude, but such cases can be recognized by examining the vertical profile of reflectivity. A radar sensitivity threshold of -30 dBZ would detect 80%, 85%, and 90% of the marine stratocumulus, with a liquid water content above 0.025, 0.05, and 0.075 g m^{-3} , respectively. Because nonprecipitating drizzle droplets are rare in continental stratocumulus, the equivalent figures are reduced to 38%, 33%, and 25%. Improving the sensitivity to -40 dBZ increases detection probability to nearly 100% for both types of cloud. These figures are based on the assumption that the cloud is deep enough to fill the radar pulse volume.

1. Introduction

Current spaceborne atmospheric monitoring systems use passive visible, infrared, and microwave measurements to observe cloud distribution and cloud-top temperatures. Millimeter-wave radar has the potential advantage over these systems of being able to penetrate multiple cloud layers and observe a complete vertical cloud structure. It has been shown (e.g., Slingo and Slingo 1991) that there is a significant lack of knowledge of the vertical cloud structure, which leads to inaccuracies in the estimation of the surface radiation budget and atmospheric radiative heating. In this paper, we consider only stratocumulus (Sc) clouds. The characteristics of cirrus clouds, as regards the ability of spaceborne radar to detect them and estimate their radiative properties, have been investigated by Brown et al. (1995) and Atlas et al. (1995); Brown et al. (1995) concluded that a sensitivity threshold of -30 dBZ was sufficient to detect radiatively significant ice clouds, whereas Atlas et al. (1995) argued that -40 dBZ was required.

By comparing multichannel measurements from the Advanced Very High Resolution Radiometer carried on

the *NOAA-9* and *NOAA-10* polar-orbiting satellites to a radiative transfer model, Han et al. (1994) have deduced cloud-top effective particle radii for a near-global set of water clouds. Nakajma and King (1990) have provided the theoretical basis for this approach. Taylor and English (1995) have derived optical depth and effective radius from radiometry and validated the technique with in situ aircraft measurements. This use of a passive radiometer seems adequate for cloud-top measurement, but it does not cope with multilayered cloud systems. A similar problem exists with the methods of Greenwald et al. (1993), who used the Special Sensor Microwave/Imager (SSM/I) aboard the Defense Meteorological Satellite Program orbiters. They derived cloud liquid water path (LWP) using a calibrated physical model applied to multichannel observations. The method chosen works only over ice-free ocean areas, and the authors point out the problems of variable sea surface emissivity caused by changes in surface conditions. Lin and Rossow (1994) have questioned the accuracy of these liquid water path retrievals.

Radar is an active system, which could penetrate cloud layers to give information on low clouds that passive instruments cannot detect due to masking by higher clouds. The major advantage of a spaceborne radar should be its ability to provide some indication of cloud thickness and base height. In order for radar to be successful in supplying the missing information, it must

Corresponding author address: Anthony J. Illingworth, Dept. of Meteorology, University of Reading, 2 Earley Gate, P.O. Box 239, Whiteknights, Reading RG6 6BB, United Kingdom.
E-mail: A.J.Illingworth@reading.ac.uk

provide a certain level of accuracy. The instrument must be capable, primarily, of detecting the majority of the radiatively significant clouds. It must be able to measure their horizontal extent and estimate their persistence accurately enough to allow radiation modelers to ascertain their effect on the earth's radiation budget (ERB). It would be beneficial if the system could also give additional information about the microphysical properties of the clouds; this possibility is discussed in Fox and Illingworth (1997).

The concerns of the study described here were, first, to discover from airborne cloud particle measurements the range of radar reflectivity factors of warm Sc clouds and hence the proportion of such clouds that a spaceborne cloud radar could detect. The second aim was to determine the accuracy with which the cloud's horizontal and vertical distribution could be measured. The role of a spaceborne cloud radar would be to complement measurements made by other instruments, such as microwave radiometers and lidars.

One system envisaged (IGPO 1994) would function at 94 GHz. The physical constraints on antenna size result in a horizontal footprint on the order of 1 km at the range of tropospheric cloud for the nadir-pointing radar. However, to achieve the target sensitivity of -30 dBZ, a 7-km (1 s) along-track integration and a vertical resolution of approximately 500 m would be required.

Sauvageot and Omar (1987), from measurements of droplet spectra in cumulus and some stratocumulus clouds over the Pyrenees, reported a relationship between the radar reflectivity and the liquid water content (LWC) of

$$Z (\text{mm}^6 \text{m}^{-3}) = 0.03 \text{LWC}^{1.31}, \quad (1)$$

where the LWC is measured in grams per cubic meter. In an equivalent study of stratocumulus clouds, Fox and Illingworth (1997) derived a relationship of the form

$$Z (\text{mm}^6 \text{m}^{-3}) = 0.031 \text{LWC}^{1.56}. \quad (2)$$

In both studies, any contribution of drizzle-sized droplets to the reflectivity was not included.

A radiatively significant stratocumulus cloud may be defined as one that leads to a significant change in visible albedo or infrared emissivity. Paltridge (1988) found that a liquid water path of only 1 g m^{-2} changed the albedo by 0.07, and an LWP of 10 g m^{-2} changed the albedo by 0.3. Chylek and Ramaswamy (1982) reported that a path of 10 g m^{-2} resulted in a broadband IR emissivity of about 0.2. Greenwald et al. (1993) presented a method of physically retrieving LWP from the SSM/I satellite, which has been widely used for deriving liquid water path cloud climatology. For cloud-free retrievals, the LWP had a standard deviation of 16 g m^{-2} , rising to about 20 g m^{-2} for cloudy areas. An adiabatic vertical profile of liquid water content increases by about 0.1 g m^{-3} per 100 m of ascent (e.g., Nicholls 1984), in which case a cloud only 50 m deep would have an average LWC of 0.025 g m^{-3} and a liquid water

path close to 1 g m^{-2} , and a 150-m-deep cloud an average LWC of 0.075 g m^{-3} with an LWP close to 10 g m^{-2} . If the LWC was 50% of the adiabatic value, then a 200-m-deep cloud with an average LWC of 0.05 g m^{-3} would have an LWP of 10 g m^{-2} . An LWP of 20 g m^{-2} could correspond to an adiabatic cloud 200 m deep with a mean LWC of 0.1 g m^{-3} or a 300-m-deep cloud with a 50% adiabatic mean LWC of 0.075 g m^{-3} .

Accordingly, in the following analysis of detectability of stratocumulus clouds, LWC threshold values of 0.025, 0.05, and 0.075 g m^{-3} will be considered, which from Eq. (2) should correspond to radar reflectivities on the order of -40 , -35 , and -32.5 dBZ, providing there are no large drops present and the cloud is deep enough to fill the pulse volume.

In the Rayleigh region, when D , the particle diameter, is much less than λ , the wavelength of the radar, the radar reflectivity Z is given by

$$Z (\text{mm}^6 \text{m}^{-3}) = \int_0^{\infty} N(D) D^6 dD, \quad (3)$$

where $N(D)$ is the concentration of drops with diameters between D and $D + dD$. From this equation, it is evident that a small number of drizzle-sized drops would dominate the reflectivity, while making a negligible contribution to the LWC. For example, a single drizzle drop $200 \mu\text{m}$ in diameter per liter would have a reflectivity of -12 dBZ but a very low LWC of only 0.04 g m^{-3} .

Nicholls (1984) reported "significant" amounts of drizzle falling from Sc 450 m thick. The significance referred to is in terms of LWC, and it can be postulated that a thinner cloud could produce enough drizzle-sized drops to dominate the radar reflectivity. Furthermore, Nicholls (1987) modeled how such drops could form in thin stratiform clouds by including turbulent effects in the growth process. Most studies of drizzle have concentrated on its ability to redistribute liquid water and its effect on cloud evolution (e.g., Albrecht 1989).

In this paper, we report on the analysis of data collected by aircraft-mounted probes, which shows that the presence of occasional drizzle-sized particles within warm Sc is far more prevalent than previously thought. These large drops serve to increase the radar reflectivity of the clouds, while having little effect on the LWC of the cloud or its radiative properties. Analysis predicts that the majority of marine Sc would be detectable by a spaceborne cloud radar, as the drizzle-sized drops tend to increase the radar reflectivity by a factor of up to 20 dBZ, compared to a similar cloud that does not contain a population of such drops.

2. Instrumentation and sampling errors

The main tools used in this work were the Particle Measuring Systems (PMS) particle probes. There is a selection of such probes flown on the Hercules C-130 aircraft of the Meteorological Research Flight (MRF).

The two principal instruments used here are the forward-scattering spectrometer probe (FSSP) and the 2D cloud (2DC) probe.

The PMS 2D cloud probe images particles with diameters of between 25 and 800 μm . The particles intercept the beam of a laser and shadow a number of photodiodes. Details of the optical and electronic configuration of the probe can be found in Knollenberg (1970). The probe sample volume varies with drop size, but with the aircraft flying at an air speed of about 100 m s^{-1} , this sample volume per second is on the order of 0.005 m^3 . This is in comparison with a typical radar pulse volume on the order of $5 \times 10^8 \text{ m}^3$. The resolution of the cloud probe is 25 μm , and the particles are sized in 32 channels of this width, up to a maximum of 800 μm . As at least half of the photodiode must be shadowed before an image is recorded, the lowest bin covers a particle size range of 12.5–37.5 μm . This channel is known to produce poor particle counts (Baumgardner 1983), and the probe is therefore not useful for the measurement of particles less than 37.5 μm in diameter.

The FSSP works by measuring the forward-scattered radiation from a laser as a particle passes into its beam (Knollenberg 1976). The FSSP measures the concentrations of particles with diameters between 2 and 47 μm , sized in 15 3- μm bins. The sample volume of the FSSP is on the order of $2 \times 10^{-5} \text{ m}^3 \text{ s}^{-1}$ at an aircraft velocity of 100 m s^{-1} . The FSSP has well-known sources of error, as has been documented by Baumgardner (1983) and Dye and Baumgardner (1984). The data processing at MRF takes into account the potential errors and corrects for the known statistically assessable errors. Sampling errors from the limited number of drops counted are discussed later and compared to these instrument-produced errors, which are on the order of 20% in both size and concentration.

a. Equations for calculating cloud parameters

The concentration of droplets in each size channel is available, corrected for the aircraft velocity. It is therefore appropriate to calculate the values of the cloud microphysical parameters Z, LWC, and effective radius r_e from the following summations:

$$Z = \sum_{i=1}^j N_i D_i^6, \quad (4)$$

$$\text{LWC} = \frac{\pi}{6} \rho \sum_{i=1}^j N_i D_i^3, \quad (5)$$

and

$$r_e = \frac{\sum_{i=1}^j N_i r_i^3}{\sum_{i=1}^j N_i r_i^2}. \quad (6)$$

In this set of equations, the sums are made over the j

TABLE 1. The errors associated with the FSSP.

	Concentration measurement uncertainties	Sizing measurement uncertainties
Precision error (%)	20	18
Bias error (%)	18	21
Total uncertainty (%)	27	28

channels of the probe being used, 15 in the FSSP probe and 32 in the 2DC. Here, N_i is the concentration of particles in the bin recording particles in a size range centered on a droplet diameter D_i or radius r_i . In practice, the first channel of each probe produces unreliable data and is not used.

When data from both probes are used in combination, it is necessary to remove the area of overlap so that particles are not counted twice. As the first 2DC probe size bin is not used, the smallest particle detected by this instrument is 37.5 μm . The twelfth FSSP channel measures particles in the size range 35–38 μm , and as the measurement uncertainties for the FSSP are greater than those for the 2DC probe because of its much smaller sample volume, it was decided to use the 2DC data rather than the measurements from the three size channels above this (i.e., channels 13, 14, and 15). When comparing measurements from the FSSP alone with those from the two instruments together, it is therefore possible to get a slightly greater, though hardly significant, measurement from the FSSP than from the two instruments combined if nothing is detected by the 2DC.

The errors associated with the measurement of particle size distributions using the FSSP are summarized in Table 1. Applying the overall uncertainty in the measurements to the calculation of Z from Eq. (4), one encounters errors on the order of 100%, as is shown later. This may appear to be a huge error, but in terms of the actual response of a radar to a cloud, this is only about 3 dBZ. Added to this in the majority of cases examined is the fact that both the radar reflectivity of the cloud and the error in this quantity are dominated by the measurement of small numbers of larger drops detected by the 2DC probe. The errors in the sizing of these larger drops is on the order of 6 μm , assuming an even distribution of the sizes of the particles recorded within each diameter range, and the error in the concentration is due to the fact that the numbers detected are very small. The Poisson errors caused by the variability of the number of drops counted are discussed below. Again, although these errors appear to be great, when expressed in dBZ, they are not burdensome.

So far we have assumed that the errors are random. However, as can be seen from Table 1, D. Baumgardner (1995, personal communication) assesses the FSSP as having bias errors that he estimates to be on the order of 20%. This bias may vary in magnitude and even sign from channel to channel, but it will be consistent from measurement to measurement. This implies a consistent

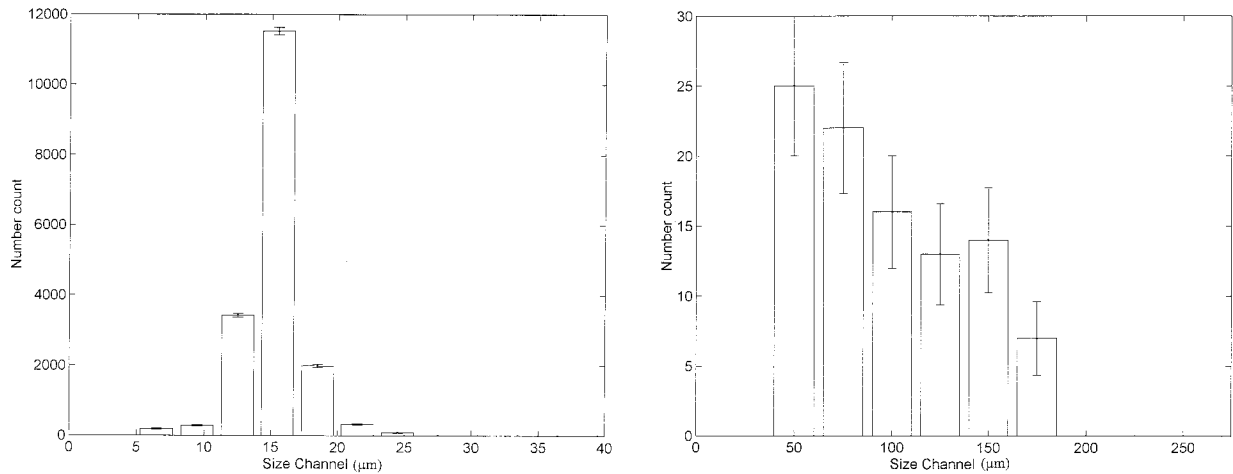


FIG. 1. (a) Droplet counts by channel measured by the FSSP for a typical 10-s period. The vertical bars represent Poisson sampling errors. (b) Drop counts by channel measured by the 2DC probe for the same period as in (a).

error in the values of cloud parameters calculated from FSSP data, which is roughly equivalent to moving a 15- μm droplet 1 channel. It is generally found that 15- μm particles are the most populous and dominate the FSSP radar reflectivity. In the worst case, this means that all the values of Z (dBZ) are biased by approximately 3 dBZ. We find that usually drizzle-sized drops are present and dominate the reflectivity, so that the errors from the FSSP make a negligible contribution.

The size ranges of the probes have been designed so that each of the PMS instruments measures a different type of hydrometeor. That is to say the FSSP detects cloud droplets and the 2DC probe images large cloud drops. This discrimination provides a ready method of separating the contributions of the different regimes to the overall properties of the cloud. Here, we define a drizzle-containing cloud as one in which the drops detected by the 2DC probe contribute as much to the reflectivity as those measured by the FSSP. We then compare the spatial dimensions of areas in which this criterion is met with the spaceborne radar's anticipated footprint.

b. Errors in finite samples

The uncertainty in the number of particles counted during a measurement is found by the application of Poisson statistics. For a finite particle count N , independent of other counts, the error σ in N is given by $N^{1/2}$. Therefore, the uncertainties in the three quantities of greatest interest are given by

$$\sigma_Z = \sum_{i=1}^j N_i^{1/2} D_i^6 = \sum_{i=1}^j (N_i D_i^{12})^{1/2}, \quad (7)$$

$$\sigma_{LWC} = \frac{\pi}{6} \rho \sum_{i=1}^j N_i^{1/2} D_i^3 = \frac{\pi}{6} \rho \sum_{i=1}^j (N_i D_i^6)^{1/2}, \quad (8)$$

and

$$\sigma_{r_e} = \left[\left(\frac{\sum N_i^{1/2} r_i^3}{\sum N_i r_i^3} \right)^2 + \left(\frac{\sum N_i^{1/2} r_i^2}{\sum N_i r_i^2} \right)^2 \right]^{1/2} r_e. \quad (9)$$

The MRF C-130 operates at a nominal air speed of 100 m s^{-1} , so in order to reduce the statistical error of the measurements and to match the spatial scale to that of the expected radar footprint (of the order of 1 km), the data were averaged over 10 s. In the actual calculation of sample volumes and particle concentrations, the aircraft's true airspeed, recorded concurrently with other in situ measurements, is used.

Examples of particle size spectra measured by the two probes and their associated Poisson errors are shown in Fig. 1. If we then wish to calculate the relative contributions to the reflectivity of the particles detected in each of the channels for each of the probes, we can do so using Eq. (4). In these equations, N_i depends not only on the number of counts in the channel, but also on the sample volume, which is quite different for each probe, being about 5 L s^{-1} for the 2DC and only 0.02 L s^{-1} for the FSSP but also varying from channel to channel and with the true airspeed of the aircraft. The sum in Eq. (4) therefore becomes

$$Z (\text{mm}^6 \text{m}^{-3}) = \sum_{i=1}^j n_i v_i^{-1} D_i^6, \quad (10)$$

where n_i is the number of particles counted in channel i and v_i is the sample volume of that channel.

Using these values, we can calculate the contribution from each size range of particles to the reflectivity, and this is shown in Fig. 2. The uncertainties in the values of Z_i are also displayed as error bars. The contributions from the top channels and their associated errors will dominate the total reflectivity. It is seen that these are on the order of 2 dBZ. This is comparable to the instrument errors described above and is acceptable in the

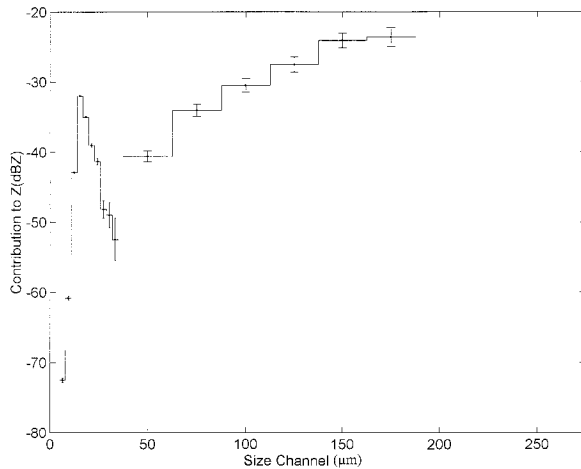


FIG. 2. Contributions to Z (dBZ) from each channel of the FSSP and 2DC probes from the drop counts in Fig. 1.

context of this investigation, where the number of individual samples of data looked at was large.

3. Data

The data used were collected during the Atlantic Stratocumulus Transition Experiment (ASTEX) and a series of flights around the coastal British Isles. ASTEX was a project designed to investigate the effect of air mass transitions on the nature of Sc. It took place in June 1992 around the area of the Azores archipelago in the North Atlantic. The other flights took place between December 1990 and February 1992. Here, the ASTEX flights are those with numbers in the A200s, whereas the other flights are those conducted around the British Isles. Table 2 summarizes the flights used. The number and cumulative length of the level runs used are shown. Data from profiles through cloud were also used to infer the nature of the radar appearance of cloud top and base. Although excellent data can be obtained from profiles for use in the study of relationships between Z and other parameters, such flight legs may not be reliable in the determination of areas of drizzle-sized droplets because

of the changing drop size distribution (DSD) as one traverses a cloud from top to bottom.

The air mass type is a broad categorization based on a combination of synoptic backtracking and subcloud aerosol concentration measurements (Martin et al. 1994). The air mass is either continental (C) or maritime (M); in some cases, it is described as basically one type but exhibiting some characteristics of the other (e.g., A169). The transitions examined in some of the ASTEX flights mean that on some days the aircraft sampled both types of cloud (A212 and A216).

4. Results

a. The frequency of drizzle-sized drops in stratocumulus

The problem addressed in this work concerns the presence of larger drops such as those found by Sauvageot and Omar (1987) in cumulus and Sc, and the impact of populations of these drops on cloud radar measurements. Although the complete formation mechanism of these drops is not well understood, it is generally believed that they form at cloud top and that low CCN concentration, the mixing of dry air, and turbulence play an important role in their development (Nicholls 1987). If these are indeed the crucial factors in the development of the DSD, then it is to be expected that the presence of areas containing drizzle-sized drops in clouds should be associated with regions of reasonably strong ascent. No investigation of the size of in-cloud areas containing occasional drizzle-sized drops has been conducted, although previous studies have noted the presence and importance of precipitating drizzle (Albrecht 1989; Nicholls and Leighton 1986).

The transverse dimensions of updrafts in Sc have been measured and seen to be on the order of 1 km (Nicholls 1984). Reports from aircraft penetrations during ASTEX repeatedly mention the intrusion of cumulus turrets into the stratiform cloud layer, and all these observations suggest the possibility that drizzle could be associated with regions of ascent on the order of 0.5–1 km across. This is consistent with the findings of Stephens and Platt

TABLE 2. The flights made by the MRF C-130 aircraft used in this study.

Flight	Date	No. of runs	Total length (km)	Approximate cloud depth (m)	Air mass (C/M)	Notes
A049	6 Dec 90	9	549.1	650	M	Off southwest England
A070	26 Feb 91	10	650.3	>350	C	North Sea
A164	10 Jan 92	7	210.8	>400	M	Off northwest Scotland
A169	5 Feb 92	9	273.2	300	C(M)	Off southwest England
A170	7 Feb 92	5	165.6	400	C	North Sea
A207	9 Jun 92	4	220.3	200	M	Cumulus intrusion
A209	12 Jun 92	7	419.3	300–550	?	
A212	16 Jun 92	5	300.3	>300	C/M	
A213	19 Jun 92	6	401.8	>200	M	Cumulus intrusion
A214	20 Jun 92	4	240.0	150	M	Some cumulus
A216	22 Jun 92	4	449.4	>400	C/M	Some cumulus

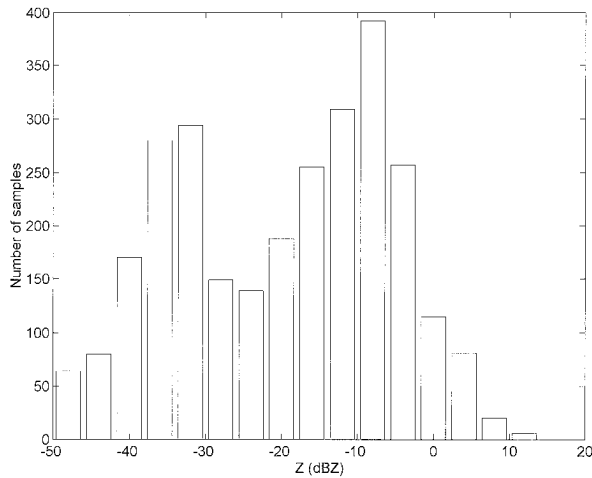


FIG. 3. The distribution of radar reflectivities of all 10-s cloud samples above -50 dBZ observed in this study.

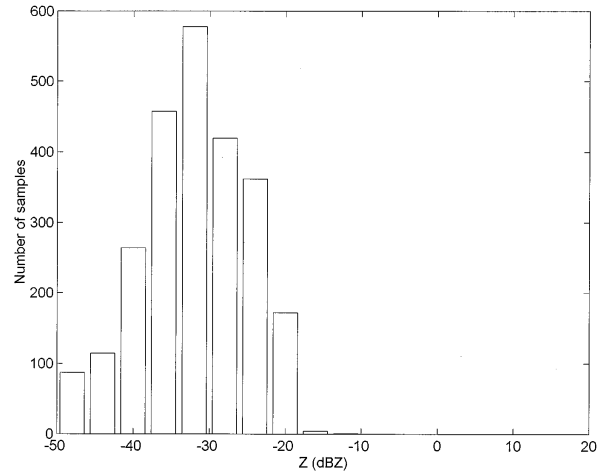


FIG. 4. The distribution of reflectivities of clouds calculated from FSSP data alone.

(1987) for stratocumulus and Paluch and Baumgardner (1989) for continental cumulus, who found peaks in LWC on the order of 1 km across associated with strong updrafts. If this were the case and the areas containing drizzle-sized drops were smaller than the along-track integration length (typically 10 km) needed to increase the sensitivity of the proposed spaceborne radar, then such drizzle areas would not be resolved, but could result in the enhancement of the radar reflectivity.

b. The range of Z for stratocumulus

The distribution of cloud sample Z values is shown in the histogram in Fig. 3, which shows that values of Z range from below -30 dBZ to above 0 dBZ, consistent with the direct observations of Z made in stratocumulus by Frisch (1995). There were 4117 samples of data examined, each corresponding to about a 1-km path in cloud; 2059 had $Z > -30$ dBZ, and 2799 had $Z > -50$ dBZ. The maximum value of radar reflectivity found for a warm Sc cloud was 13.7 dBZ. There are two maxima in the frequency distribution (Fig. 3) of the cloud reflectivities at the intervals -38 to -30 dBZ and -10 to -6 dBZ. Figure 4 shows the frequency distribution of cloud reflectivity calculated from FSSP measurements alone; the removal of the drizzle component results in data points being transferred from high Z bins to lower Z bins. In this case, the maximum sample reflectivity found is -10.9 dBZ and the modal value in the -34 to -30 dBZ range is clear, showing that this is the reflectivity for the underlying cloud droplet spectrum. This is further emphasized if one considers the histogram (Fig. 5) for flight A169, which is the only case in which no population of drizzle-sized drops was observed. The maximum sample reflectivity is -27.8 dBZ, and the modal reflectivity is once again seen to be in the -38 to -30 dBZ range. This confirms that

the bimodal distribution of cloud reflectivities is caused by the particles detected by the 2DC probe.

The values of LWC and Z for the 2799 samples with Z greater than -50 dBZ are plotted in Fig. 6, in which the two different symbols correspond to samples taken from clouds formed in continental and maritime air masses. The three vertical lines correspond to the threshold LWC values of 0.025 , 0.05 , and 0.075 g m^{-3} , as discussed in section 1. Histograms showing the range of Z values calculated for the two types of Sc are shown in Fig. 7. As can be seen, the maximum reflectivity factor for the continental clouds is much lower (1.9 dBZ) than that for the maritime cases. These maritime clouds produce a maximum Z of 13.7 dBZ and a significant number (145) of 10-s samples with Z greater than 0 dBZ. The maritime cases have a large modal Z value of about -8 dBZ and a weaker one at about -32 dBZ, whereas for the continental cases, the magnitude of the

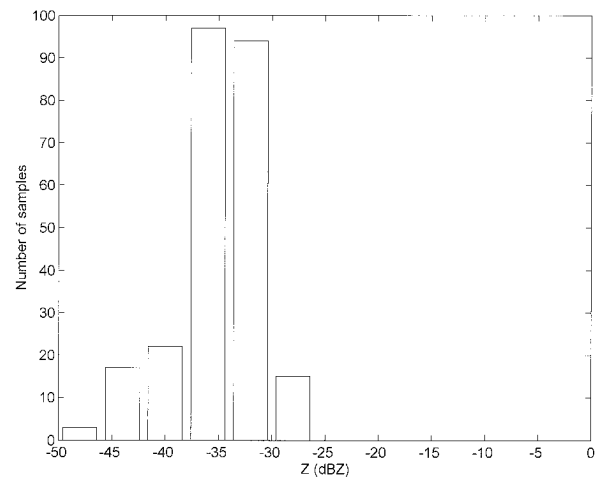


FIG. 5. As in Fig. 3 but for flight A169 (continental aerosol) only.

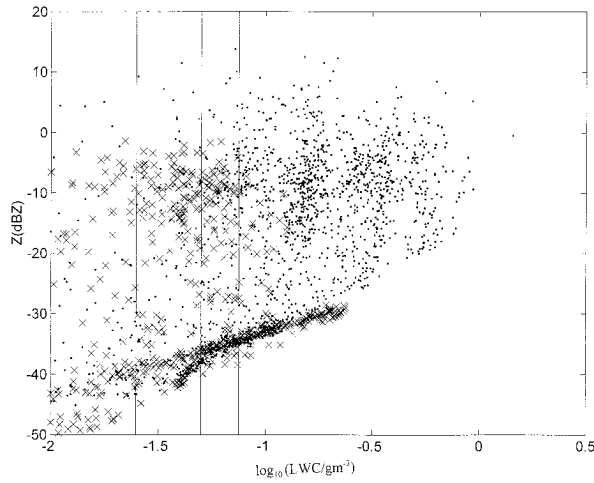


FIG. 6. Scattergram of calculated Z against LWC for all maritime (dots) and continental (crosses) Sc samples with $Z > -50$ dBZ. The three vertical lines are for the 0.025 , 0.050 , and 0.075 g m^{-3} values of LWC.

modal frequency of sample Z at -32 dBZ is greater than that at -8 dBZ.

The data in Fig. 6 are summarized in Table 3a, where the fraction of data points exceeding the three LWC threshold values is shown for various possible Z thresholds between -30 and -40 dBZ. This analysis is also carried out with a further subdivision into marine and continental air masses. In the case of the marine air mass (Table 3b), a Z threshold of -30 dBZ detects 80%, 85%, and 90% of all data with LWCs above 0.025 , 0.05 , and 0.075 g m^{-3} , respectively. Examination of the data points classified as marine below the -30 -dBZ threshold reveals that they are found on occasions when the origin of the air mass was uncertain, when the clouds were thinner than 200 m , or when the in-cloud pene-

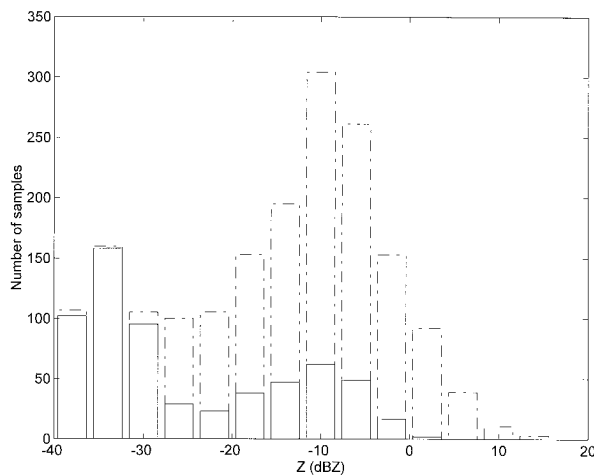


FIG. 7. The result of separating the reflectivities into those calculated for maritime (broken line) and continental (unbroken line) cloud.

TABLE 3a. The percentage of data points exceeding a liquid water content threshold for various Z thresholds. Final column is the total number of data points. Data are from all air masses.

dBZ	Liquid water content threshold		
	0.025 g m^{-3}	0.05 g m^{-3}	0.075 g m^{-3}
> -40	98	100	100
> -37.5	93	96	100
> -35	86	93	99
> -32.5	77	82	91
> -30	70	75	82
All	2142	1787	1425

trations were only a few km long and a knowledge of the cloud's nature was incomplete. Reducing the Z threshold for the marine clouds to -40 dBZ resulted in virtually 100% detection.

The situation for the continental air mass (Table 3c) is rather different. For a threshold of -30 dBZ, only 38%, 33%, and 25% of all data with LWCs above 0.025 , 0.05 , and 0.075 g m^{-3} , respectively, were detected. Increasing the sensitivity to -40 dBZ yields 100% detection apart from the 0.025 g m^{-3} case, where it is 95%. In all cases, it is assumed that the cloud fills the radar pulse volume; this may not be valid for very thin clouds, in which case a lower Z threshold would be needed.

Figure 6 reveals that for the majority of data points the presence of occasional drizzle-sized droplets means that Z is not correlated with LWC, so that there is no obvious use of quantitative values of Z . LWC is proportional to D^3 , and the rainfall rate for this size range of the droplets is proportional to D^4 . So, in view of the very wide scatter of the LWC contribution to Z of the drizzle droplets, the value of Z is not related to the precipitation rate of the drizzle droplets.

c. The horizontal distribution of areas containing drizzle-sized drops

From the data examined, taken from 70 straight level runs amounting to over 4000 km of horizontal flying, it appears that marine Sc clouds almost always contain drizzle-sized drops. Here, a "significant amount of drizzle-sized drops" is defined as a quantity that contributes as much to the value of Z ($\text{mm}^6 \text{ m}^{-3}$) as the underlying population of cloud droplets—that is, Z ($\text{mm}^6 \text{ m}^{-3}$) is

TABLE 3b. As for Table 3a but for only marine air masses.

dBZ	Liquid water content threshold		
	0.025 g m^{-3}	0.05 g m^{-3}	0.075 g m^{-3}
> -40	99	100	100
> -37.5	95	99	100
> -35	91	95	99
> -32.5	85	89	95
> -30	80	85	90
All	1523	1380	1193

TABLE 3c. As for Table 3a but for only continental air masses.

dBZ	Liquid water content threshold		
	0.025 g m ⁻³	0.05 g m ⁻³	0.075 g m ⁻³
> -40	95	100	100
> -37.5	86	98	100
> -35	72	82	97
> -32.5	53	54	64
> -30	38	33	25
All	528	336	182

at least doubled, corresponding to an increase in Z (dBZ) of 3 dBZ. It is suggested that this effect has previously gone unnoticed, as the amount of drizzle present is very small in terms of LWC, but because Z is proportional to the sixth moment of drop diameter, it is far more sensitive to the presence of a few larger droplets.

Figure 8 shows a typical time series for Z and LWC from a straight-level aircraft run. The unbroken line is the parameter calculated from the entire drop spectrum, while the broken line shows that due only to the cloud DSD as measured by the FSSP alone. The cloud edge can be seen in both parameters at a range of 50 km. It is apparent that Z is raised by about 15 dBZ, while LWC is unchanged by the presence of the occasional drizzle-sized drops. These features are seen not only in the example shown in Fig. 8, but repeatedly in all of the clouds studied that contained occasional drizzle drops. Drizzle-sized drops, of significance in terms of the radar reflectivity factor, are found throughout the entire horizontal extent of the cloud and do not occur in small localized patches of size comparable to that of the radar footprint.

The one day upon which the quantity of drizzle encountered never fulfilled this criterion was the day of

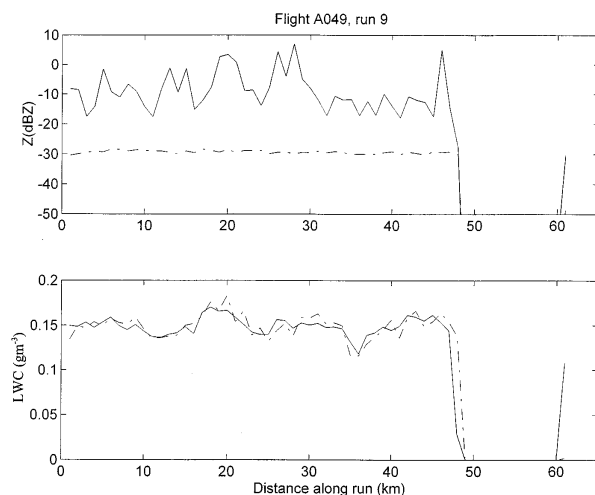


FIG. 8. Typical time series for Z and LWC for a penetration of a cloud containing occasional drizzle drops. The dotted line shows the parameters calculated for the underlying population of cloud droplets measured by the FSSP alone.

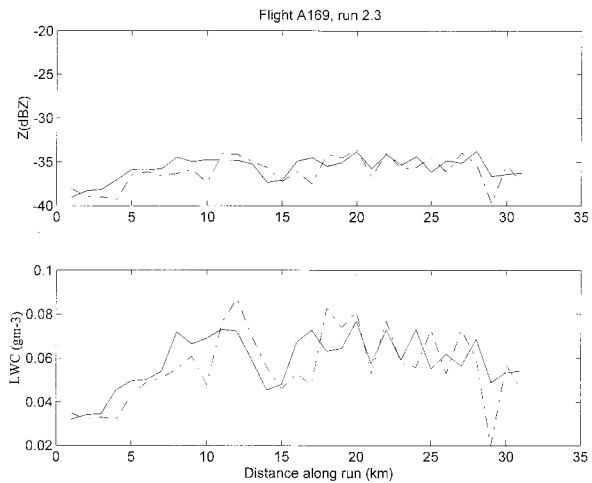


FIG. 9. As in Fig. 8 but for a drizzle-free cloud.

flight A169, and a typical time series for a run during this flight is shown in Fig. 9. The cloud observed during this flight was predominantly continental in nature, and CCN concentrations of 700 cm⁻³ were measured.

d. The vertical distribution of drizzle-sized drops

The vertical distribution of drizzle-sized drops could be derived from the 29 aircraft profiles that have not been included in the analysis discussed so far. Drizzle-sized drops are found throughout the vertical extent of the clouds studied. An example of this is shown in Fig. 10. The data for this graph are taken from a profile through the thick Sc found during flight A049, run 1.2. The values of both Z and LWC due to the cloud droplets are shown by the dashed line, and that for the entire drop spectrum is shown by the solid line. There are drizzle-sized drops throughout the cloud, and these

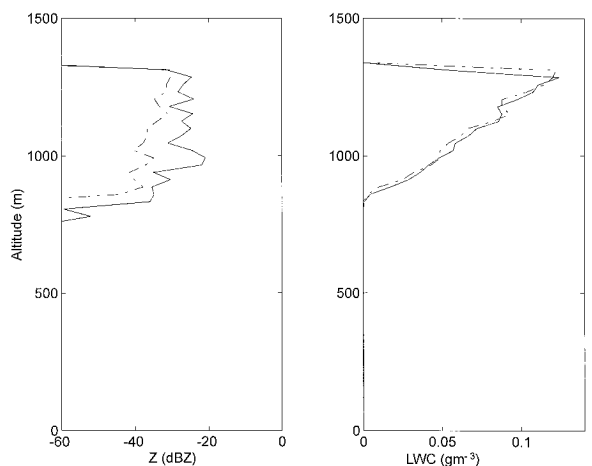


FIG. 10. Typical vertical profile in Z and LWC from an aircraft profile through a cloud containing occasional drizzle drops. The dotted line shows the parameters calculated from FSSP data alone.

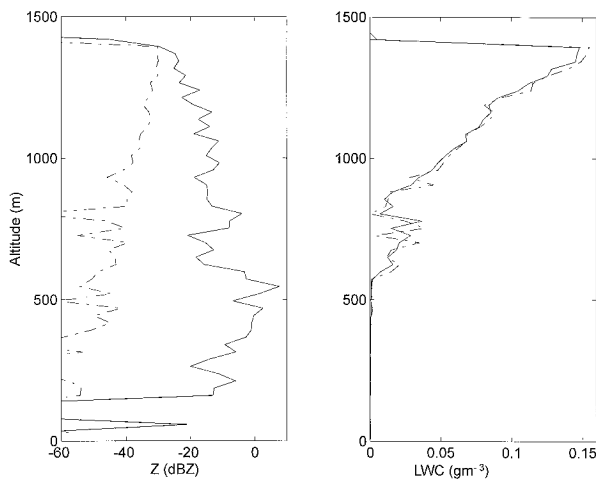


FIG. 11. As in Fig. 10 but for a thicker cloud that has slight drizzle falling below cloud base.

drops dominate the radar reflectivity, but they contribute negligibly to the LWC. It appears that the droplet size distribution is changed very little by either collision or diffusion processes, and Z at cloud base is almost unchanged from that at cloud top. This contrasts with the extreme case displayed in Fig. 11 from the same flight, run 2.2. In this profile, the reflectivity increases as the drops that are initially larger than those in run 1.2 grow by collision and coalescence as they fall through the body of the cloud. The drizzle in this case falls about 500 m below cloud base before evaporating.

While the reflectivity factor behaves in this manner, LWC, although subadiabatic, increases consistently as one rises through the cloud, as has been observed on numerous occasions (e.g., Martin et al. 1994). Below cloud base, the falling drops observed during run 1.2 evaporate rapidly in the unsaturated air. Figures 12 and 13 illustrate the differences in the development of DSDs between the two cases. In the case of run 1.2, the drops are initially small and rarely exceed $200\ \mu\text{m}$. In contrast in run 2.2 (Fig. 13), the presence of large drops (over $400\ \mu\text{m}$ in diameter) persists from the cloud top throughout the cloud, and these drops then fall about 500 m below the cloud base. This is consistent with our knowledge of the fall speeds and evaporation rates of drops—for this size of droplet, the terminal velocity is proportional to its diameter, so the distance a droplet survives a fall from cloud base increases rapidly with the third power of the diameter if the relative humidity is constant. For example, with 70% humidity, a $200\text{-}\mu\text{m}$ -diameter drizzle droplet falls 25 m, and a 0.5-mm -diameter droplet 400 m, before total evaporation.

It is apparent from looking at the 29 profiles that an increase in Z with cloud height is an indicator that the drizzle-sized drops are not growing sufficiently to fall a significant distance below cloud base before evaporating. On the other hand, decreasing Z with height seems to be an indicator that the falling drops are grow-

ing and may precipitate far enough to give a false measurement of cloud base by a spaceborne radar. It is possible that in cases in which there are returns from three (or more) gates and the reflectivity decreases with altitudes, it can be assumed that drizzle is falling a significant distance below the cloud. In this event, cloud base height should be corrected.

To summarize, in the clouds in which drizzle-sized drops are found, they are present throughout the depth of the cloud. They serve to increase the reflectivity of the cloud so that it becomes easy to detect using the proposed cloud radar. In most cases, the quantity of drizzle is insignificant in liquid water terms and does not change much through the depth of the cloud. As it falls from the base of the cloud, the drizzle evaporates rapidly. The lowering of the apparent cloud base, as it would be measured by radar, is generally much smaller than the vertical resolution (500 m) of the spaceborne radar and would rarely lead to any increased error in cloud-base estimation. In a small number of cases when the cloud is particularly thick, the drizzle formed grows significantly during its descent through the cloud, enhancing the reflectivity of the lower portion of the cloud. These larger drizzle drops fall farther below the cloud before evaporating and are likely to give a false measure of cloud-base altitude. The distinctive pattern of higher reflectivity toward cloud base than at cloud top could lead to identification of such cases. Coupled with this, the greater thickness of these clouds and the drizzle itself are likely to produce detectable radar returns from three gates, giving the appearance of an Sc cloud more than 1 km thick. This should be a notable occurrence and should provide some means of correcting for the effects of below-cloud drizzle on radar reflectivity.

5. Attenuation

In discussing the radar reflectivity of warm clouds, one must consider the possible attenuation of the signal as it passes through a volume containing liquid water. Lhermitte (1988) quotes the attenuation at 94 GHz due to absorption in the Rayleigh regime at $4\ \text{dB km}^{-1}\ (\text{g m}^{-3})^{-1}$, while Clothiaux et al. (1995) give a slightly lower figure. For a cloud 500 m thick with an LWC of $0.5\ \text{g m}^{-3}$, the two-way attenuation would be about 2 dB, provided that all the particles are Rayleigh scatterers for a 3-mm wavelength. Figure 6 predicts that clouds with such high values of LWC have reflectivities above $-20\ \text{dBZ}$, so the 2-dB attenuation should not impact the cloud detectability threshold. Recently, T. Ackerman (1995, personal communication) has shown some results, taken with the ground-based, vertically pointing, Pennsylvania State University 94-GHz cloud radar, which reveal areas of high reflectivity ($> -10\ \text{dBZ}$) at low altitudes that are not associated with attenuation (as seen from the reflectivities of higher clouds). This can be explained by the presence of drizzle-sized particles in the lower stratiform clouds.

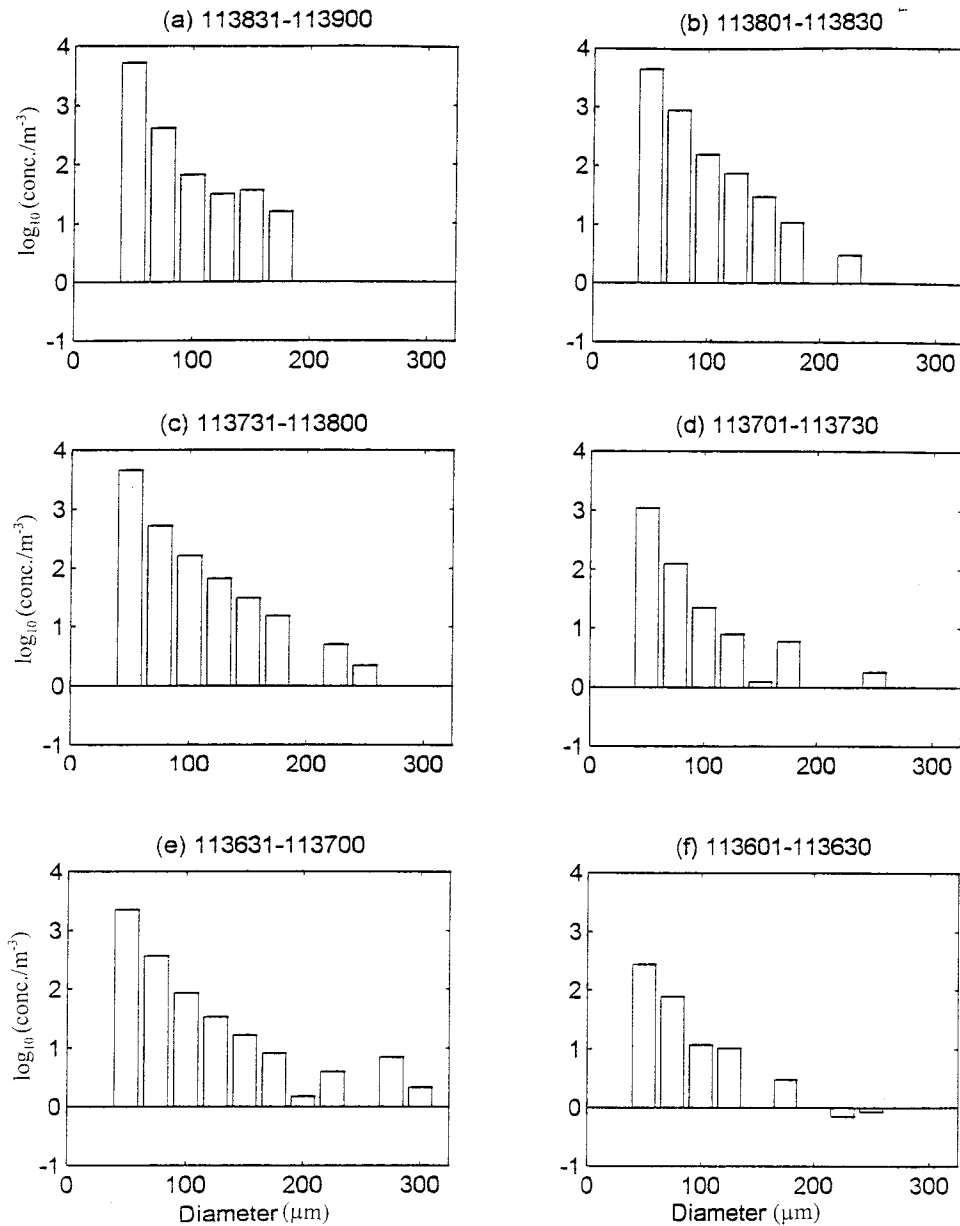


FIG. 12. Drop concentrations measured for the profile in Fig. 10. (a) The DSD at cloud top and (f) that at cloud base. Each spectrum is separated by about 75 m in the vertical.

6. Conclusions

The main points revealed by this study are as follows.

- 1) Drizzle-sized particles are prevalent in warm marine Sc and are sometimes found in continental Sc. They can be absent in marine Sc thinner than about 200 m and in broken marine Sc.
- 2) These drizzle-sized particles, although insignificant in terms of the LWC and the radiative properties of the cloud, serve to raise the radar reflectivity of the cloud. This makes the clouds easier to detect, but means that the value of Z is not related to the LWC.
- 3) The drizzle-sized drops are present throughout the cloud and appear to be bounded only by the cloud edge. They are also found throughout the vertical depth of the cloud but should usually evaporate within 200 m of cloud base.
- 4) A radar sensitivity threshold of -30 dBZ would detect 80%, 85%, and 90% of marine Sc with LWCs above 0.025 , 0.05 , and 0.075 g m^{-3} ; these values correspond to LWPs of between 1 and 20 g m^{-2} . The equivalent figures for continental Sc are only 38%, 33%, and 25%. Increasing the sensitivity to -40 dBZ increases the detection probability to near-

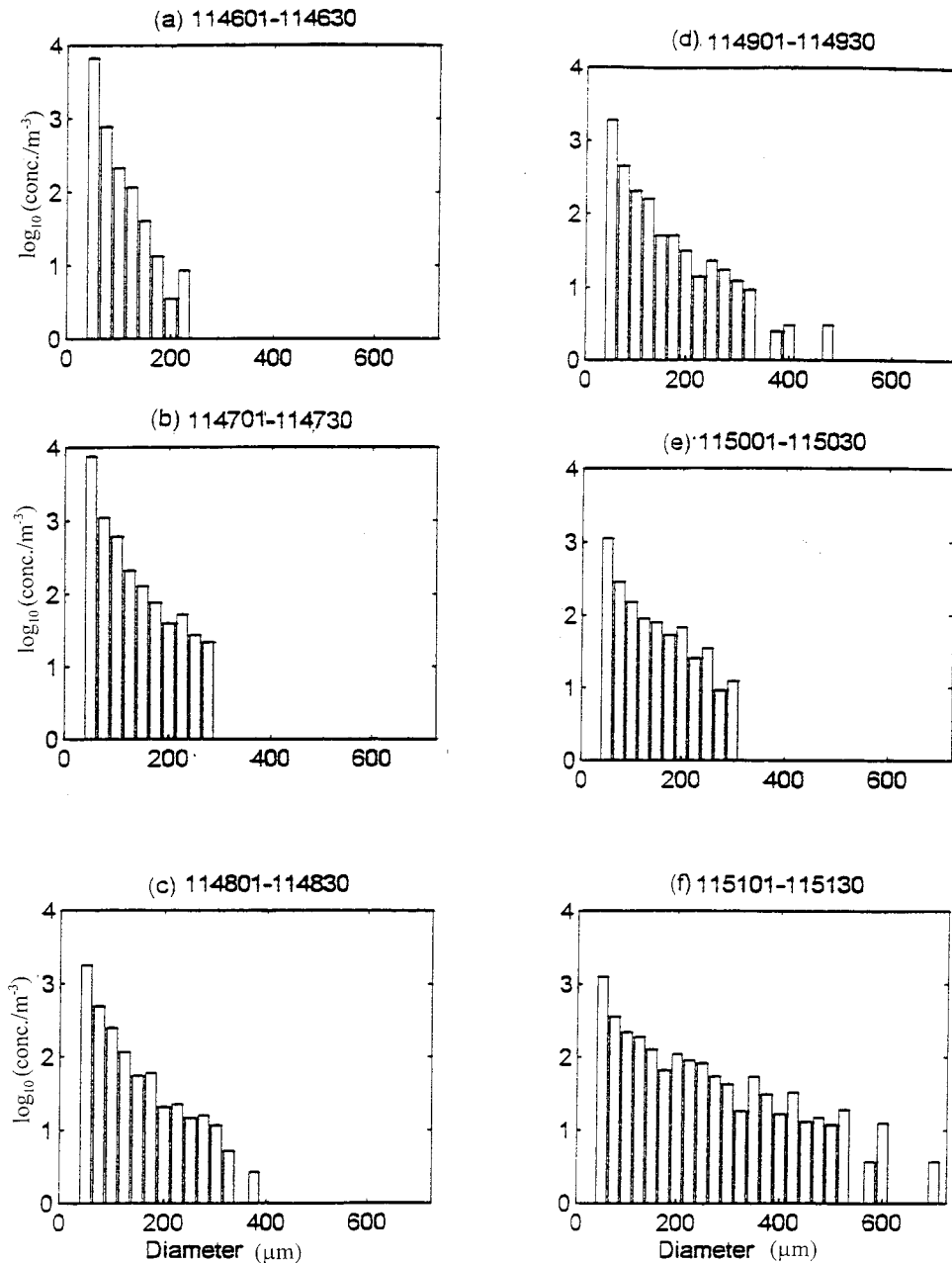


FIG. 13. DSDs for the profile in Fig. 11. (a) From cloud top and (d) from cloud base. The vertical separation of the spectra is 150 m. In contrast to Fig. 12, it is seen that a population of initially larger drops grows as one descends through the cloud, and the resulting drops fall a substantial distance below cloud base. In (f), some very large drops are observed; this is likely to be caused by a horizontal variation.

ly 100% for both continental and marine clouds. These figures assume that the pulse volume is completely filled with clouds. Increases in sensitivity would be needed to detect thin clouds not filling the pulse volume.

- 5) If the liquid water path is high enough to cause significant attenuation of the 94-GHz radar signal, then the cloud invariably contains drizzle-sized drops, which raise the reflectivity above -20 dBZ; as a

result, attenuation does not affect the threshold values of Z needed to detect stratocumulus clouds.

There is a need to further investigate both the distribution of areas of cloud containing drizzle-sized drops and their reflectivities. There is a fair quantity of aircraft probe data that have already been taken around the world in both continental and maritime Sc. The examination of such data would increase knowledge of

how the findings presented in this paper compare to other situations. In particular, if there were more data to divide by cloud type, cloud age, and geographical location, it is possible that important variations could be found under different conditions. Similarly, as the processes that are believed to lead to the production of larger drops involve the effects of entrainment and radiation, it would be illuminating to see if there is a noticeable change between day- and nighttime clouds. Ideally, the findings of this study require verification with coincident aircraft and cloud radar measurements.

Acknowledgments. We thank the Meteorological Research Flight for supplying the aircraft data and P. R. A. Brown for assistance with the data processing. This work was supported by NERC Grant GR3/8765, ESTEC Grant 10568/93, and CEC Environment Programme EV5V-CT-94-0463.

REFERENCES

- Albrecht, B. A., 1989: Aerosols, cloud microphysics and fractional cloudiness. *Science*, **245**, 1227–1230.
- Atlas, D., S. Y. Matrosov, A. J. Heymsfield, M.-D. Chou, and D. B. Wolff, 1995: Radar and radiation properties of ice clouds. *J. Appl. Meteor.*, **34**, 2329–2345.
- Baumgardner, D., 1983: An analysis of five water droplet measuring instruments. *J. Climate Appl. Meteor.*, **22**, 891–910.
- Brown, P. R. A., A. J. Illingworth, A. J. Heymsfield, G. M. McFarquhar, K. A. Browning, and M. Gosset, 1995: The role of spaceborne millimeter-wave radar in the global monitoring of ice cloud. *J. Appl. Meteor.*, **34**, 2346–2366.
- Chyleck, P., and V. Ramaswamy, 1982: Simple approximation for infrared emissivity of water clouds. *J. Atmos. Sci.*, **39**, 171–177.
- Clothiaux, E. E., M. A. Miller, B. A. Albrecht, T. P. Ackerman, J. Verlinde, D. M. Babb, R. M. Peters, and W. J. Syrett, 1995: An evaluation of a 94-GHz radar for remote sensing of cloud properties. *J. Atmos. Oceanic Technol.*, **12**, 201–229.
- Dye, J. E., and D. Baumgardner, 1984: Evaluation of the forward scattering spectrometer probe. Part I: Electronic and optical studies. *J. Atmos. Oceanic Technol.*, **1**, 329–344.
- Fox, N. I., and A. J. Illingworth, 1997: The retrieval of stratocumulus cloud properties by ground-based cloud radar. *J. Appl. Meteor.*, **36**, 485–492.
- Frisch, A. S., D. H. Lenschow, C. W. Fairall, W. H. Schubert, and J. S. Gibson, 1995: Doppler radar measurements of turbulence in marine stratiform cloud during ASTEX. *J. Atmos. Sci.*, **52**, 2800–2808.
- Greenwald, T. J., G. L. Stephens, T. H. Vonder Haar, and D. L. Jackson, 1993: A physical retrieval of cloud liquid water over the global oceans using Special Sensor Microwave/Imager (SSM/I) observations. *J. Geophys. Res.*, **98**, 18 471–18 488.
- Han, Q., W. B. Rossow, and A. A. Lacis, 1994: Near-global survey of the effective droplet radii in liquid water clouds using ISCCP data. *J. Climate*, **7**, 465–497.
- IGPO, 1994: *Utility and Feasibility of a Cloud Profiling Radar*. IGPO Publication Series, Vol. 10, International GEWEX Program Office, 140 pp.
- Knollenberg, R. G., 1970: The optical array: An alternative to scattering or extinction for airborne particle size determination. *J. Appl. Meteor.*, **9**, 86–103.
- , 1976: Three new instruments for cloud physics measurements: The 2D spectrometer, the forward scattering spectrometer probe, and the active scattering aerosol spectrometer. Preprints, *Int. Conf. on Cloud Physics*, Boulder, CO, Amer. Meteor. Soc., 554–561.
- Lhermitte, R. M., 1988: Cloud and precipitation remote sensing at 94 GHz. *IEEE Trans. Geosci. Remote Sens.*, **26**, 207–216.
- Lin, B., and W. B. Rossow, 1994: Observations of cloud liquid water path over oceans: Optical and microwave sensing methods. *J. Geophys. Res.*, **99**, 20 907–20 927.
- Martin, G. M., D. W. Johnson, and A. Spice, 1994: The measurement and parameterization of effective radius of droplets in warm stratocumulus clouds. *J. Atmos. Sci.*, **51**, 1823–1842.
- Nakajima, T., and M. D. King, 1990: Determination of the optical thickness and effective particle radius of clouds from reflected solar radiation measurements. Part I: Theory. *J. Atmos. Sci.*, **47**, 1878–1893.
- Nicholls, S., 1984: The dynamics of stratocumulus: Aircraft observations and comparisons with a mixed layer model. *Quart. J. Roy. Meteor. Soc.*, **110**, 783–820.
- , 1987: A model of drizzle growth in warm, turbulent, stratiform clouds. *Quart. J. Roy. Meteor. Soc.*, **113**, 1141–1170.
- , and J. Leighton, 1986: An observational study of stratiform cloud sheets: Part I. Structure. *Quart. J. Roy. Meteor. Soc.*, **112**, 431–460.
- Paltridge, G., 1988: Spectral and total albedo to solar radiation of ice and water clouds—Experimental results from ASPIRE. *Atmosfera*, **1**, 5–16.
- Paluch, I. R., and D. G. Baumgardner, 1989: Entrainment and fine-scale mixing in a continental convective cloud. *J. Atmos. Sci.*, **46**, 261–278.
- Sauvageot, H., and J. Omar, 1987: Radar reflectivity of cumulus clouds. *J. Atmos. Oceanic Technol.*, **4**, 264–272.
- Slingo, A. J., 1990: Sensitivity of the earth's radiation budget to changes in low clouds. *Nature*, **343**, 49–51.
- Stephens, G. L., and C. M. R. Platt, 1987: Aircraft observations of the radiative and microphysical properties of stratocumulus and cumulus cloud fields. *J. Climate Appl. Meteor.*, **26**, 1243–1269.
- Taylor, J. P., and S. J. English, 1995: The retrieval of cloud radiative and microphysical properties using combined near-infrared and microwave radiometry. *Quart. J. Roy. Meteor. Soc.*, **121**, 1083–1112.